Sphingosylphosphorylcholine Induces Apoptosis of Endothelial Cells Through Reactive Oxygen Species-Mediated Activation of ERK

Eun Su Jeon,[1] Mi Jeong Lee,[1] Sang-Min Sung,[2] and Jae Ho Kim[1]*

[1]Medical Research Center for Ischemic Tissue Regeneration & Medical Research Institute, College of Medicine, Pusan National University, Busan 602-739, Republic of Korea
[2]Department of Neurology, Busan Medical Center, Busan 611-072, Republic of Korea

Abstract Sphingosylphosphorylcholine (SPC) produces reactive oxygen species (ROS) in MS1 pancreatic islet endothelial cells. In the present study, we explored the physiological significance of the SPC-induced ROS generation in endothelial cells. SPC induced cell death of MS1 cells at higher than 10 μM concentration through a caspase-3-dependent pathway. SPC treatment induced sustained activation of an extracellular signal-regulated kinase (ERK), in contrast to transient activation of ERK in response to platelet-derived growth factor (PDGF)-BB, which stimulated proliferation of MS1 cells. Both the SPC-induced cell death and ERK activation were abolished by pretreatment of the cells with the MEK inhibitor U0126 or by overexpression of a dominant negative mutant of MEK1 (DN-MEK1). Pretreatment of the cells with *N*-acetylcysteine, an antioxidant, completely prevented the SPC-induced ROS generation, apoptosis, and ERK activation, whereas the ROS generation was not abrogated by treatment with U0126. Consistent with these results, SPC induced cell death of human umbilical vein endothelial cells (HUVECs) through ROS-mediated activation of ERK. These results suggest that the SPC-induced generation of ROS plays a crucial role in the cell death of endothelial cells through ERK-dependent pathway. J. Cell. Biochem. 100: 1536–1547, 2007. © 2006 Wiley-Liss, Inc.

Key words: sphingosylphosphorylcholine; reactive oxygen species; ERK; apoptosis; endothelial cells

Sphingosylphosphorylcholine (SPC) has been implicated in a number of biological processes,

including proliferation, growth inhibition, smooth muscle contraction, wound healing, and angiogenesis [Meyer zu Heringdorf et al., 2002]. SPC stimulates proliferation of various cell types, such as fibroblasts, endothelial cells, keratinocytes, and vascular smooth muscle cells [Desai and Spiegel, 1991; Sun et al., 1996; Chin and Chueh, 1998; Wakita et al., 1998; Meyer zu Heringdorf et al., 2002]. On the other hand, it can also inhibit growth of various cell types, mostly tumor cells, such as pancreatic, breast, and ovarian cancer cells and Jurkat T cells [Yamada et al., 1997; Xu, 2002]. In the vascular system, SPC induces migration and morphogenesis of vascular endothelial cells in vitro [Boguslawski et al., 2000]. These results indicate that SPC may be involved in vascular physiology or pathophysiology via modulation of growth, viability, and differentiation of endothelial cells. However, the molecular mechanisms involved in the SPC-induced growth control are still unclear.

Reactive oxygen species (ROS) have been implicated in the regulation of growth and cell

death in vascular endothelial cells. In support of the above contention, we recently reported that SPC treatment stimulated the production of ROS in MS1 pancreatic islet endothelial cells [Jeon et al., 2005a]. Furthermore, treatment of endothelial cells with exogenous H_2O_2 caused apoptotic cell death [de Bono and Yang, 1995]. In addition, endogenous H_2O_2 produced by oxidized low density lipoprotein (LDL) induced endothelial cell death [Lin et al., 2004]. Therefore, by modulating endothelial cell growth and apoptosis, ROS seems to be involved in a variety of cardiovascular diseases, such as atherosclerosis and hypertension [Stoneman and Bennett, 2004; Touyz and Schiffrin, 2004; Cai, 2005; Schulze and Lee, 2005]. However, the physiological significance of ROS in SPC-induced cellular responses has not yet been studied.

Mitogen-activated protein kinases (MAPKs), which include the extracellular signal-regulated kinase (ERK), c-Jun NH_2-terminal protein kinase, and p38 MAPK, are involved in the regulation of cellular processes, such as cell growth, differentiation, development, cell cycle, death, and survival [Chang and Karin, 2001]. Several studies demonstrated that ERK is involved mainly in the regulation of proliferation. SPC has been shown to enhance ERK activity in various cell lines [Meyer zu Heringdorf et al., 2002; Xu, 2002], and the SPC-induced activation of ERK has been reported to be essential for the SPC-induced cell death in human adipose tissue-derived mesenchymal stem cells (hATSCs) [Jeon et al., 2005b]. However, the molecular mechanisms by which ROS and ERK regulate the SPC-induced cell death of endothelial cells have not yet been addressed. In the present study, we demonstrate for the first time that ROS plays a key role in the SPC-induced cell death of endothelial cells through ERK-dependent pathway.

MATERIALS AND METHODS

Materials

D-erythro-SPC and L-threo-SPC were purchased from Matreya (Pleasant Gap, PA). U0126, pertussis toxin (PTX) z-VAD-FMK, and DEVE-CHO were from BIOMOL (Plymouth Meeting, PA). Dulbecco's Modified Eagle's Medium and LipofectAMINE were from Invitrogen (Carlsbad, CA), and fetal bovine serum was from HyClone (Logan, UT). Human umbilical vein endothelial cells (HUVECs), endothelial growth medium (EGM-2) Bullet kit, and EBM-2 basal medium were purchased from Cambrex Corp. (East Rutherford, NJ). Anti-phospho-ERK, anti-ERK, and anti-cleaved caspase-3 antibodies were obtained from Cell Signaling Technology, Inc. (Beverly, MA). The anti-actin antibody (clone C4) and horseradish peroxidase-conjugated secondary antibodies were from MP Biomedicals (Irvine, CA) and Jackson ImmunoResearch Lab. (West Grove, PA), respectively. The enhanced chemiluminescence kit was from Amersham Biosciences (Buckinghamshire, UK). Dichlorodihydrofluorescein diacetate (H_2DCF-DA) was purchased from Molecular Probes, Inc. (Eugene, OR). 3-(4,5-dimethylthiazol-2-yl)-2,5-diphenyltetrazolium bromide (MTT), N-acetylcysteine (NAC), and all other reagents were from Sigma-Aldrich Co. (St. Louis, MO).

Cell Culture and Transient Transfection

MS1 cells, pancreatic islet endothelial cells transformed by infection with a temperature sensitive SV40 large T antigen (tsA-58-3), were purchased from American Type Culture Collection (Manassas, VA). They were maintained in a high glucose Dulbecco's Modified Eagle's Medium, supplemented with 25 mM $NaHCO_3$, 10% fetal bovine serum, 50 U/ml penicillin, and 50 μg/ml streptomycin, in a 5% CO_2/95% O_2 humidified incubator at 37°C. HUVECs were cultured for up to eight passages in an EGM-2 BulletKit, and the growth medium was replaced with endothelial basal medium for serum deprivation before treatment with SPC. For transient overexpression of a dominant negative mutant of MEK1 (DN-MEK1), a mammalian expression vector (pCGN) bearing DN-MEK1 was transfected into MS1 cells with LipofectAMINE, as suggested by the manufacturer (Invitrogen).

Cell Viability Assay

Cell viability was determined by MTT assay, as described previously [Alley et al., 1988]. For the MTT assay, the stock solution (5 mg/ml MTT) was added to each well of the 96-well plates, which were seeded with MS1 cells, to a final concentration of 0.5 mg/ml MTT, and then the plates were incubated at 37°C for 2 h. The formazan granules generated by live cells were dissolved in 100% dimethylsulfoxide (DMSO) and absorbance at 570 nm was monitored by

using a PowerWave$_x$ microplate spectrophotometer (Bio-Tek Instruments, Inc., Winooski, VT). For direct counting of viable cell number, the reagents-treated hADSCs were harvested by trypsinization, suspended in phosphate-buffered saline, and incubated with an equal amount of 0.1% trypan blue. The number of trypan blue-negative cells was counted by using a hemocytometer.

TUNEL Staining

Cells were grown on 22-mm glass coverslips in six-well plates. After treatment with SPC, cells were washed twice with PBS and fixed with 4% paraformaldehyde in PBS (pH 7.4) for 1 h at 4°C. The fixed cells were stained by the terminal deoxynucleotidyl transferase-mediated dUTP nick-end labeling (TUNEL) method, using an in situ cell death detection Kit (Roche, Basel, Switzerland), as described in the manufacturer's manual: the DNA cleavage generated during apoptosis is labeled at strand breaks with fluorescein dUTP by terminal deoxynucleotidyl transferase. Fluorescence of the labeled fluorescein was excited at 485 ± 11 nm and emitted fluorescence was collected at 530 ± 15 nm. The fluorescence, indicating DNA strand breaks, and phase contrast images were photographed by a digital camera equipped in an inverted microscope (Leica DM IRB).

Flow Cytometric Analysis

Cell cycle was analyzed by fluorescence-activated cell sorting after staining with propidium iodide. Cells were collected by centrifugation, washed with PBS, and permeabilized in 70% ethanol, containing 0.5% Tween 20, overnight at 4°C. The permeabilized cells were incubated with 50 μg/ml propidium iodide and 0.1 mg/ml RNase A (Sigma) for 30 min at 37°C and analyzed for apoptosis. Cells with sub-G_1 propidium iodide incorporation were considered as apoptotic, and the percentage of apoptotic cells was calculated as the ratio of events on sub-G_1 to events from the whole population.

Western Blot Analysis

Confluent serum-starved cells were treated under the appropriate conditions as specified, washed with ice-cold PBS, and then lysed in lysis buffer [20 mM Tris-HCl (pH 7.4), 1 mM EGTA, 1 mM EDTA, 10 mM NaCl, 0.1 mM phenylmethanesulfonyl fluoride,

1 mM Na_3VO_4, 30 mM sodium pyrophosphate, 25 mM β-glycerol phosphate, and 1% Triton X-100]. Lysates were resolved by SDS–PAGE and transferred onto a nitrocellulose membrane. After blocking with 5% non-fat milk, the membranes were immunoblotted with various antibodies, and the bound antibodies were visualized with horseradish peroxidase-conjugated rabbit IgG antibodies by using the enhanced chemiluminescence Western blotting system.

Measurement of ROS

Intracellular ROS production was measured by the method of Bass et al. [1983] with a slight modification of a previous report [Ohba et al., 1994]. Briefly, cells were seeded onto 32 mm dishes and serum-starved for 24 h. The serum-starved cells were treated with SPC for 30 min and loaded with 20 μM H_2DCF-DA for 10 min. Fluorescence formed as a result of the oxidation of dichlorodihydrofluorescein (excitation, 488 nm; emission, 515–540 nm) to a fluorescent derivative, DCF, was measured by confocal microscopy, using a Leica TCS-SP2 laser scanning confocal microscope (Leica Microsystems, Germany). Photo-oxidation of dichlorodihydro-fluorescein was minimized by collecting the fluorescent image with a single rapid scan (line average, 4; total scan time, 4.33 s) using identical parameters, such as contrast and brightness, for all samples.

RESULTS

SPC Decreases the Viability of MS1 Cells

To explore the effects of SPC on viability and proliferation of MS1 cells, cell number was determined by using an MTT assay. As shown in Figure 1A, treatment of MS1 cells with D-*erythro*-SPC for 48 h dose-dependently decreased the cell number. To assess whether the SPC-induced cell death was due to the detergent-like property of SPC, we compared the effect of SPC stereo-isomers on the cell viability. In contrast to D-*erythro*-SPC-induced cell death, treatment of the cells with L-*threo*-SPC had no significant impact on the viability of MS1 cells, indicating that D-*erythro*-SPC stereo-selectively induced cell death of MS1 cells. To confirm the result that D-*erythro*-SPC stereo-selectively decreased the viability of MS1 cells, we next measured the cell number by using a hemocytometer and cell viability was assessed
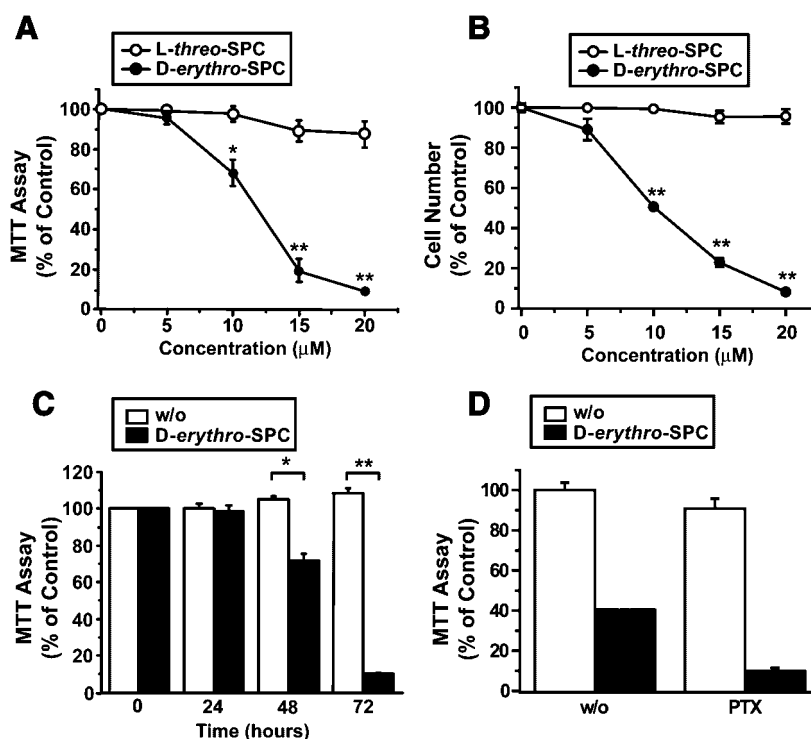
Fig. 1. Effects of exogenous SPC on cell viability of MS1 cells. Serum-starved MS1 cells were treated with indicated concentrations of D-erythro-SPC or L-threo-SPC for 48 h. The cell number was determined by MTT assay (**A**) or trypan blue exclusion assay (**B**). **C**: Serum-starved MS1 cells were treated with vehicle (0.1% DMSO) or 10 µM D-erythro-SPC for the indicated periods of time. **D**: Serum-starved MS1 cells were pretreated with 100 ng/ml PTX or vehicle for 24 h and then treated with vehicle (0.1% DMSO) or 10 µM D-erythro-SPC for 48 h. Cell viability was determined by MTT assay and expressed as a percentage of control. Data are shown as mean ± SE (n = 4). Representative data of three independent experiments are shown. *, $P < 0.05$ and **, $P < 0.01$.

by trypan blue exclusion. Consistent with the result determined by MTT assay, D-erythro-SPC stereo-selectively decreased the viable cell number (Fig. 1B). The SPC-induced cell death became apparent after 48 h of exposure of MS1 cells to 10 µM D-erythro-SPC, and the cell viability decreased time dependently (Fig. 1C). The stereo-selective response of SPC on cell viability of MS1 cells suggest that D-erythro-SPC probably causes cell death of MS1 endothelial cells via a stereo-specific plasmalemmal receptor.

In a previous study, we demonstrated that SPC stimulated proliferation of hATSCs through a PTX-sensitive G protein-sensitive pathway [Jeon et al., 2006]. Therefore, we next explored whether the SPC-induced death of MS1 cells is mediated by PTX-sensitive G proteins. As shown in Figure 1D, the SPC-induced death of MS1 cells was not ameliorated by PTX treatment, suggesting that PTX-sensitive G proteins, G_i or G_o, are not involved in the SPC-induced death of MS1 cells.

Involvement of Caspase-3-Dependent Pathway in SPC-Induced Apoptosis

To explore whether SPC induces apoptotic cell death of MS1 cells, we next investigated the effects of SPC on cell cycle and DNA strand breaks. As shown in Figure 2A, SPC treatment increased the percentage of the sub-G_1 phase, which is a hallmark of apoptosis, from 5.2% (control) to 18.3% (SPC-treated cells). In addition, TUNEL-positive apoptotic cells, which manifest DNA strand breaks or DNA fragmentation during apoptosis, appeared in the MS1 cells treated with D-erythro-SPC for 48 h, but not in control cells (Fig. 2B, upper panels). Incubation with D-erythro-SPC for 48 h also induced drastic morphological change of MS1 cells (Fig. 2B, lower panels), which coincides with the TUNEL-positive cells. Therefore, these results indicate that SPC-induced cell death occurred primarily through apoptotic pathways.

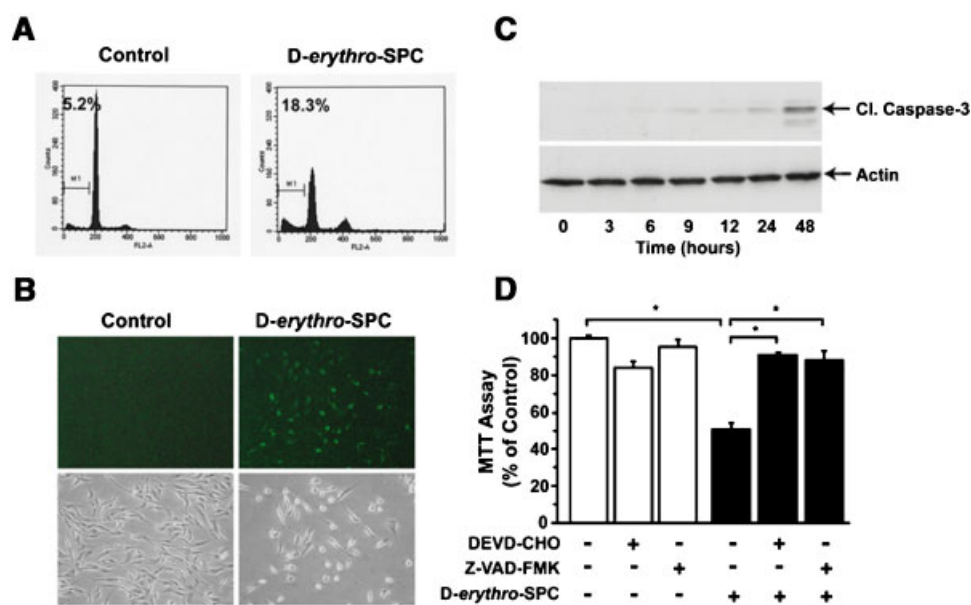It is well known that cytochrome c release from mitochondria to cytosol leads to activation

Fig. 2. Role of caspase-3 in SPC-induced apoptotic cell death. **A**: For analysis of the cell cycle, serum-starved MS1 cells were pretreated with vehicle or 10 μM D-*erythro*-SPC for 48 h, and then labeled with propidium iodide. Propidium iodide (PI)-labeled cells (~10,000 events) were analyzed by a FACscan flow cytometer using the cell Quest software to quantitate a sub-G_1 cell population. **B**: Serum-starved MS1 cells were treated with vehicle or 10 μM D-*erythro*-SPC for 48 h, fixed, and stained with a TUNEL assay kit, as described under Materials and Methods. Fluorescence and phase contrast images are shown in upper and lower panels, respectively. Representative data of three independent experiments are shown. **C**: Serum-starved MS1 cells were treated with 10 μM D-*erythro*-SPC for the indicated times, and the amounts of cleaved caspase-3 in an aliquot (40 μg) of cytosolic fractions were determined by Western blotting with an anti-cleaved caspase-3-specific antibody. The amounts of actin were probed by an anti-actin antibody to confirm equal loading. Representative data of three independent experiments are shown. **D**: Serum-starved MS1 cells were pretreated with vehicles (0.1% DMSO), 10 μM DEVD-CHO, the caspase-3 specific inhibitor, and 20 μM z-VAD-FMK, the general caspase inhibitor, for 15 min, and then treated with 10 μM D-*erythro*-SPC for 48 h as indicated. Cell viability was determined by MTT assay and expressed as a percentage of control (Mock-incubated cells). Data are shown as mean ± SE (n = 4) and are representative of three independent experiments. * Indicates $P < 0.05$. [Color figure can be viewed in the online issue, which is available at www. interscience.wiley.com.]

of caspase cascades: Cytochrome *c*-dependent cleavage of caspase-3 leads to its activation, and thus activated caspase-3 plays a key role in apoptosis by proteolysis of various cellular proteins [Jiang and Wang, 2004]. To explore whether the activation of caspase-3 was involved in the SPC-induced apoptosis of MS1 cells, we examined the effect of SPC on cleavage of caspase-3. As shown in Figure 2C, cleavage of caspase-3 appeared after treatment of the cells with 10 μM SPC for 12 h, and maximally occurred after 48 h. To further clarify whether caspase-3 was involved in SPC-induced cell death, we next examined the role of caspase-3 in SPC-induced apoptosis. As shown in Figure 2D, SPC treatment reduced the cell viability, and pretreatment of the cells with either 10 μM EDVD-CHO, a caspase-3-specific inhibitor, or 20 μM z-VAD-FMK, a general caspase inhibitor, completely restored SPC-induced cell viability. These data indicate that

the caspase-3-dependent pathway plays a crucial role in SPC-induced apoptosis.

ERK Is Involved in the SPC-Induced Apoptosis of MS1 Cells

We have previously reported that ERK activation is required for SPC-induced cell death in hATSCs [Jeon et al., 2005b]. However, it is generally accepted that ERK is involved in proliferation in response to mitogenic growth factors acting through receptor protein tyrosine kinase or G protein-coupled receptors [Chang and Karin, 2001]. To explore the role of ERK in SPC-induced cell death and the growth factor-induced proliferation of endothelial cells, we determined the effects of U0126, a specific inhibitor of MEK1/2, on the viability of MS1 cells treated with 10 μM D-*erythro*-SPC or 10 ng/ml platelet-derived growth factor (PDGF). As shown in Figure 3A, pharmacological inhibition of ERK by pretreatment of MS1 cells with
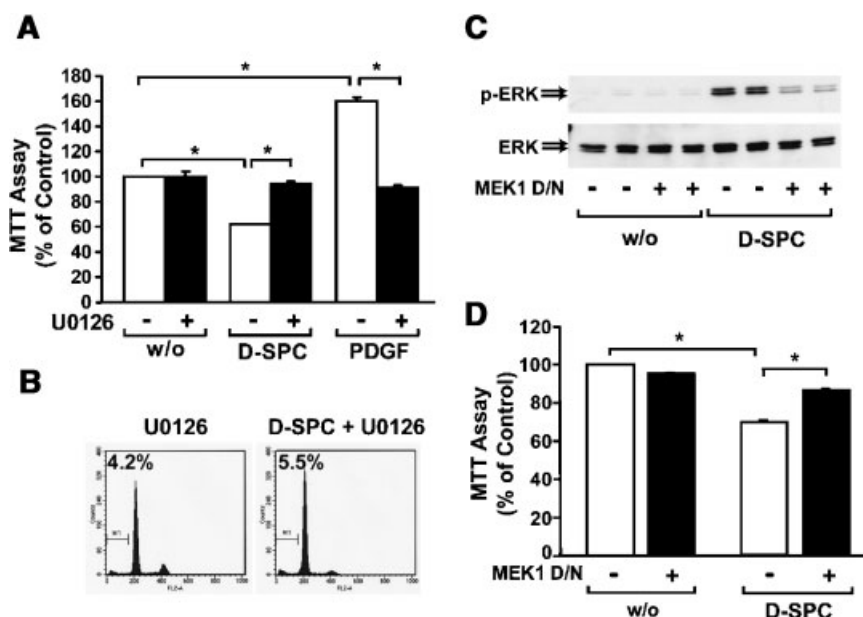
Fig. 3. Role of ERK in SPC-induced cell death and PDGF-induced proliferation. **A:** Serum-starved MS1 cells were pretreated with vehicles or 10 μM U0126 for 15 min, and then exposed to 10 μM D-erythro-SPC (D-SPC) or 10 ng/ml PDGF-BB (PDGF) for 48 h. Cell number was determined by MTT assay and expressed as a percentage of control (Mock-incubated cells). Data are shown as mean ± SE (n = 4) and are representative of three independent experiments. * Indicates $P < 0.05$. **B:** Serum-starved MS1 cells were pretreated with 10 μM U0126, exposed to 10 μM D-erythro-SPC or vehicle for 48 h, and then labeled with PI. Propidium iodide (PI)-labeled cells (∼10,000 events) were analyzed by a FACscan flow cytometer using the cell Quest software to quantify a sub-G_1 cell population. Representative data of three independent experiments are shown. MS1 cells were transfected with pCGN-DN-MEK1 or a control vector, and then treated with vehicle or 10 μM D-erythro-SPC for 30 min. Representative data of three independent experiments in duplicated determinations are shown. **C:** MS1 cells were transfected with pCGN-DN-MEK1 or a control vector, and then treated with vehicle or 10 μM D-erythro-SPC for 48 h. Phosphorylation levels of ERK1/2 and the amounts of ERK1/2 were determined by Western blotting with anti-phospho-ERK1/2 and anti-ERK antibodies, respectively. **D:** Cell number was determined by MTT assay and values are expressed as a percentage of mock-treated cells. Data are shown as mean ± SE (n = 4) and are representative of three independent experiments. *, $P < 0.05$.

U0126 markedly abrogated SPC-induced cell death. Furthermore, PDGF increased the cell number of MS1 cells and the PDGF-induced proliferation was completely prevented by pretreatment of the cells with U0126. These results suggest that ERK plays a key role in both SPC-induced cell death and PDGF-induced proliferation of MS1 cells.

To ascertain the involvement of ERK in the D-erythro-SPC-induced apoptosis, we investigated the effect of U0126 on the SPC-induced increase of sub-G_1 phase DNA contents. Treatment of MS1 cells with 15 μM D-erythro-SPC increased the percentage of the sub-G_1 fraction from 5.2% (control cells, Fig. 2A) to 18.3% (SPC-treated cells, Fig. 2A), and pretreatment of MS1 cells with U0126 drastically decreased the percentage of the sub-G_1 phase DNA contents to 5.5% (Fig. 3B).

To further confirm the involvement of the MEK-ERK pathway in SPC-induced apoptosis, we next explored the effects of DN-MEK1 on the SPC-induced apoptosis and phosphorylation of ERK in MS1 cells, and found that overexpression of the DN-MEK1 significantly attenuated the SPC-induced phosphorylation of ERK (Fig. 3C). Moreover, SPC-induced apoptosis was significantly abrogated by overexpression of the DN-MEK1 (Fig. 3D), supporting the conclusion that ERK plays a pivotal role in the SPC-induced apoptosis of MS1 cells.

SPC Induces Prolonged Activation of ERK in MS1 Cells

To determine the molecular mechanisms by which both SPC-induced apoptosis and PDGF-induced proliferation are mediated by ERK, we examined the effects of SPC and PDGF on ERK phosphorylation in MS1 cells. Treatment of MS1 cells with PDGF-induced robust phosphorylation of ERK as early as 10 min, and then it was rapidly declined to the basal level at 30 min. SPC also induced phosphorylation of ERK at 10 min, whereas the phosphorylated

level of ERK was slowly decreased as compared with the PDGF-induced ERK phosphorylation. The ERK phosphorylation could be detected at 24 h after treatment of the cells with SPC, but not with PDGF (Fig. 4A,B). Pretreatment of MS1 cells with U0126 completely inhibited the ERK phosphorylation induced by SPC or PDGF. These results suggest that SPC-induced cell death of MS1 cells by inducing prolonged activation of ERK, in contrast to short-lived activation of ERK induced by PDGF.

SPC-Stimulated Generation of ROS Is Required for the SPC-Induced Apoptosis Through ERK-Dependent Pathway

We have recently reported that SPC treatment increased intracellular levels of ROS in MS1 cells [Jeon et al., 2005a]. To assess the
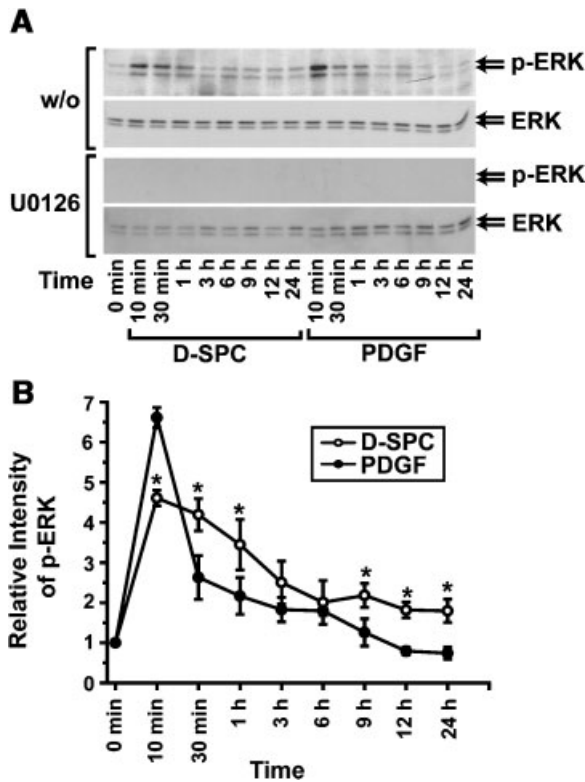

Fig. 4. Time-dependent Effects of SPC and PDGF on the ERK Phosphorylation. **A**: Serum-starved MS1 cells were pretreated with vehicles or 10 µM U0126, and then treated with 10 µM D-erythro-SPC (D-SPC) or 10 ng/ml PDGF-BB (PDGF) for the indicated time periods. Phosphorylation levels of ERK1/2 and the amounts of ERK1/2 were determined by Western blotting with anti-phospho-ERK1/2 and anti-ERK antibodies, respectively. Representative data of three independent experiments are shown. **B**: The densities of p-ERK and ERK were quantified from the three experiments, and the phosphorylation levels of p-ERK were normalized to the amounts of ERK in the samples. Data are shown as mean ± SE ($n = 3$). *, $P < 0.05$ (D-SPC vs. PDGF-BB).

role of ROS in SPC-induced ERK activation, we examined the effects of N-acetylcysteine (NAC), an antioxidant, on SPC-induced ROS generation and activation of ERK. As shown in Figure 5A, the SPC-induced generation of ROS was prevented by pretreatment of MS1 cells with NAC. However, pretreatment of the cells with U0126 did not block the SPC-induced ROS generation. In order to demonstrate the role of ROS in the SPC-induced activation of ERK, we next examined the effect of NAC on the SPC-induced phosphorylation of ERK in MS1 cells. Pretreatment of MS1 cells with 1 mM NAC prevented the SPC-induced phosphorylation of ERK (Fig. 5B), indicating that SPC-induced ROS generation is essential for ERK activation in MS1 cells. To assess whether ROS plays any critical role in the SPC-induced cell death, we determined the effects of NAC on the SPC-induced cell death. Pretreatment of MS1 cells with NAC completely abrogated the SPC-induced cell death (Fig. 5C), suggesting that SPC-induced production of ROS is required for the cell death of MS1 cells.

SPC Induces Cell Death of HUVECs Through ROS-Dependent Activation of ERK

Because MS1 cells are pancreatic islet endothelial cells transformed by infection with a temperature sensitive SV40 large T antigen, it is possible that the signaling pathways involved in the SPC-induced cell death of MS1 cells may be different from those of primary endothelial cells. To confirm whether SPC causes cell death of primary endothelial cells through the ROS-ERK pathway, we next examined the effect of SPC on proliferation or cell viability of HUVECs. As shown in Figure 6A, D-erythro-SPC slightly increased the proliferation of HUVECs with a maximal stimulation at 5 µM concentration. However, a higher concentration than 10 µM D-erythro-SPC dose-dependently attenuated the viability of HUVECs. In contrast to D-erythro-SPC, L-threo-SPC treatment had no significant impact on the cell number of HUVECs, suggesting that D-erythro-SPC positively or negatively regulates the proliferation of HUVECs, depending on the concentrations of SPC exposed to the cells.

In the present study, we showed that SPC attenuated viability of MS1 cells through $G_{i/o}$-independent pathway (Fig. 1D). Therefore, we next examined the involvement of $G_{i/o}$-dependent pathway in the SPC-induced
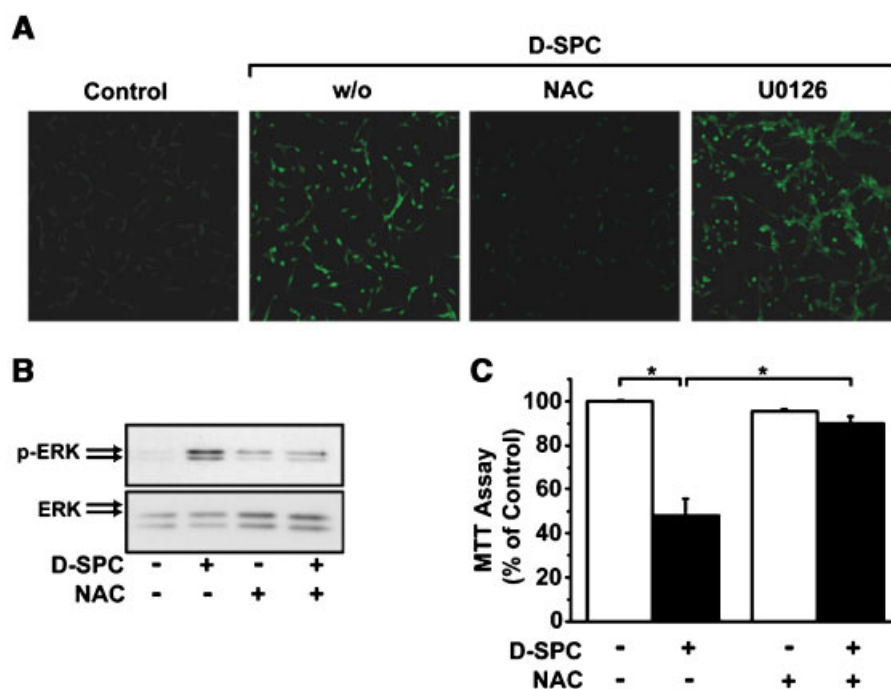
Fig. 5. Role of ROS in SPC-induced cell death. **A**: MS1 cells were pretreated with vehicle, 10 μM U0126 or 1 mM NAC for 30 min, and then treated with vehicle or 10 μM D-erythro-SPC for 30 min. The cells were then loaded with 20 μM H$_2$DCF-DA for 10 min, and fluorescence resulting from the oxidation of dichlorodihydrofluorescein to DCF was measured by the confocal microscopic procedure as described under Materials and Methods. Excitation was delivered at 485 ± 11 nm, and emitted fluorescence was collected at 530 ± 15 nm. Representative data of three independent experiments are shown. **B**: Serum-starved MS1 cells were pretreated with vehicle or 1 mM NAC for 30 min, and then exposed to 10 μM D-erythro-SPC for 30 min. Cell lysates were loaded onto 10% SDS–PAGE, and phosphorylation of ERK1/2 and the amounts of ERK were determined by Western blotting with anti-phospho-ERK1/2 and anti-ERK antibodies, respectively. Representative data of three independent experiments are shown. **C**: Serum-starved MS1 cells were pretreated with vehicle or 1 mM NAC for 30 min, and then exposed to 10 μM D-erythro-SPC for 48 h. Cell viability was determined by MTT assay. Values are expressed as a percentage of mock-treated cells. Data are shown as mean ± SE ($n = 4$) and are representative of three independent experiments. *, $P < 0.05$. [Color figure can be viewed in the online issue, which is available at www.interscience.wiley.com.]

cellular responses of HUVECs. As shown in Figure 6B, the increased proliferation of HUVECs induced by 5 μM SPC was completely abrogated by PTX treatment. Furthermore, the reduced viability of HUVECs induced by 15 μM SPC was also ameliorated by pretreatment of the cells with PTX. These results clearly suggest that SPC modulates proliferation or viability of HUVECs through G$_{i/o}$-dependent pathway, in contrast to the crucial role of G$_{i/o}$-independent pathway in the SPC-induced cell death of MS1 cells.

To discern whether ROS-dependent ERK activation was involved in the SPC-induced cell death of HUVECs, we determined the effects of U0126 and NAC on the SPC-induced phosphorylation of ERK. Treatment of HUVECs with SPC-induced phosphorylation of ERK, and pretreatment of the cells with either U0126 or NAC completely prevented the SPC-induced

phosphorylation of ERK (Fig. 6C). We next confirmed the involvement of ROS-dependent activation of ERK in the SPC-induced death of HUVECs, by determining the effects of U016 and NAC on the SPC-induced cell death of HUVECs. As shown in Figure 6D, treatment of HUVECs with SPC in the presence of U0126 ameliorated SPC-induced cell death. Furthermore, NAC completely blocked the SPC-induced cell death of HUVECs. These results indicate that the SPC-induced production of ROS plays a pivotal role in the SPC-induced endothelial cell death through activation of ERK.

DISCUSSION

In the present study, we demonstrated that SPC dose-dependently induced apoptotic cell death in MS1 transformed pancreatic islet endothelial cells (Fig. 1A). Consistently, SPC
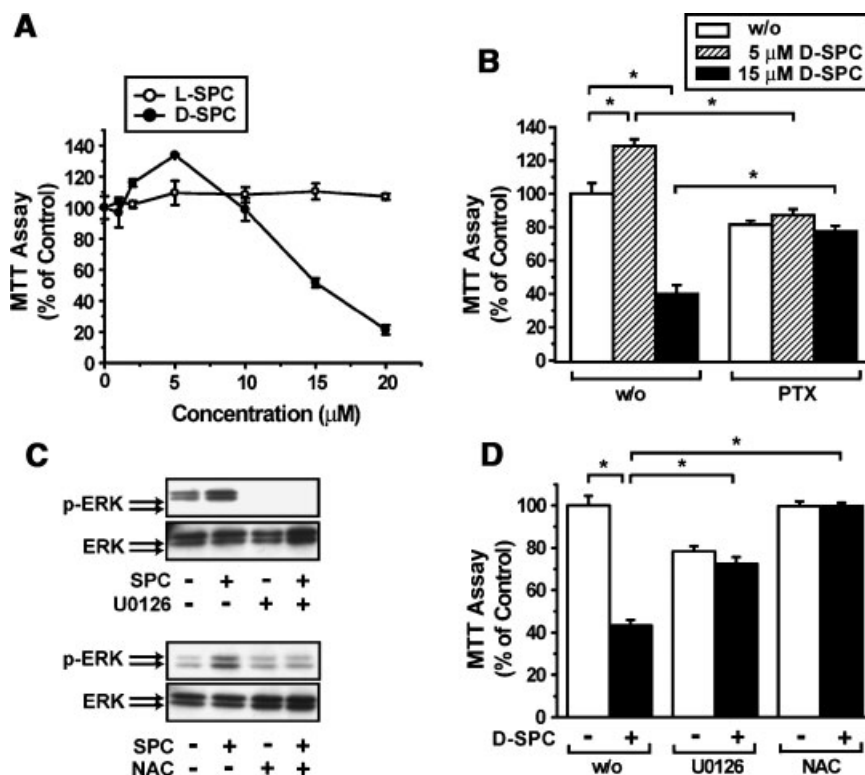
Fig. 6. Role of ROS and ERK in SPC-induced cell death of HUVECs. **A:** HUVECs were cultured in a serum-free medium in the presence of indicated concentrations of D-erythro-SPC or L-threo-SPC for 48 h, and cell number was determined by MTT assay. Data are shown as mean ± SE (n = 4) and are representative of three independent experiments. **B:** Serum-starved HUVECs were pretreated with 100 ng/ml PTX, and then treated with 5 µM or 15 µM D-erythro-SPC for 48 h. Cell number was determined by MTT assay. Data are shown as mean ± SE (n = 4) and are representative of three independent experiments. **C:** Serum-starved HUVECs were pretreated with 10 µM U0126 or

1 mM NAC for 30 min, and then exposed to vehicles or 15 µM D-erythro-SPC for 30 min. Phosphorylation levels of ERK1/2 and amounts of ERK1/2 were determined by Western blotting with anti-phospho-ERK1/2 and anti-ERK antibodies, respectively. Representative data of three independent experiments are shown. **D:** HUVECs were pretreated with 10 µM U0126 or 1 mM NAC for 30 min, and then exposed to 15 µM D-erythro-SPC for 48 h. Cell number was determined by MTT assay and values are expressed as a percentage of mock-treated cells. Data are shown as mean ± SE (n = 4) and are representative of three independent experiments. *, $P < 0.05$.

has been reported to inhibit growth of various cell types, mostly tumor cells, such as pancreatic, breast, and ovarian cancer cells or Jurkat T cells [Xu et al., 1995a,b; Yamada et al., 1997]. However, SPC induced the proliferation of HUVECs with a maximal stimulation at 5 µM, whereas concentrations of SPC greater than 10 µM induced the cell death of HUVECs (Fig. 6A). The biphasic effect of SPC on proliferation has previously been observed in non-transformed cell types, such as keratinocytes, Swiss 3T3 fibroblast, and hATSCs [Desai et al., 1993; Wakita et al., 1998; Jeon et al., 2005b, 2006]. A possible explanation for the cell type-specific effects of SPC is that different signaling pathways contribute to the differential effects of SPC. In the present study, we demonstrated that the biphasic effect of SPC on proliferation of

HUVECs was mediated by $G_{i/o}$-dependent pathway, in contrast to the involvement of $G_{i/o}$-independent pathway in the SPC-induced cell death of MS1 cells. These results suggest that distinct signaling mechanisms involving $G_{i/o}$-dependent and -independent pathways are responsible for the differential effects of SPC on proliferation or death in these endothelial cells. Another possibility is that the differential effects of SPC are due to differential expression of SPC receptors. Several GPCRs, such as OGR1, GPR4, G2A, and GPR12, have been identified as high affinity receptors for SPC [Meyer zu Heringdorf et al., 2002; Xu, 2002]. Recently, Kim et al. [2005] demonstrated that GPR4 is involved in the SPC-induced angiogenesis and proliferation in HUVECs. In addition, sphingosine-1-phosphate (S1P) receptors have

been reported to act as low affinity receptors for SPC [Meyer zu Heringdorf et al., 2002; Xu, 2002]. Moreover, SPC has been identified previously as an anti-apoptotic agent in HUVECs [Nofer et al., 2001] and the S1P receptor $S1P_3$ (also known as LPB_3 and EDG_3) has been reported to play a crucial role in the SPC-induced signal transduction [Nofer et al., 2004]. Therefore, it is highly likely that differential expression of these SPC receptors is responsible for the differential effects of SPC on proliferation and apoptosis in MS1 cells and HUVECs. However, accumulating evidence has recently demonstrated that OGR1, GPR4, and G2A are activated by proton, but not by SPC [Bektas et al., 2003; Ludwig et al., 2003; Murakami et al., 2004]. Therefore, it is still unclear which receptors are involved in the SPC-induced proliferation or death of HUVECs. Furthermore, it has been reported that autotaxin, a member of the nucleotide pyrophosphatase/PDE family of ecto/exoenzymes, hydrolyzes SPC to produce S1P [Clair et al., 2003]. Because S1P stimulates proliferation of human endothelial cells through PTX-sensitive pathway [Wang et al., 1999; Kimura et al., 2000], it is plausible that S1P, which is produced by autotaxin-mediated hydrolysis of SPC, stimulates proliferation of HUVECs through activating the S1P receptor-$G_{i/o}$-dependent pathway. Additional studies are needed to understand the precise role of these receptors and signal transduction pathways involved in the SPC-induced proliferation and apoptosis.

In the present study, we demonstrated that prolonged activation of ERK was responsible for the cell death of MS1 cells induced by a high concentration of SPC; however, PDGF stimulated proliferation of MS1 cells by inducing acute activation of ERK (Figs. 3 and 4). The above contention is further supported by a few recent studies that the MEK-ERK-dependent pathway is involved in the induction of apoptosis [Lieu et al., 1998; Kalechman et al., 2000; Kim et al., 2003; Nguyen et al., 2004], in contrast to previous reports that ERK plays a crucial role as an anti-apoptotic factor [Chang and Karin, 2001; Wada and Penninger, 2004]. The opposite roles of ERK in apoptosis might possibly be explained by the fact that ERK plays a dual role in the regulation of cell death and survival, depending on the strength and duration of its activation: Persistent activation of ERK leads to cell death [Stanciu et al., 2000;

Seo et al., 2001; Canals et al., 2003], whereas a short-lived activation of ERK is associated with survival [Xia et al., 1995; Fukunaga and Miyamoto, 1998]. In addition, ERK stimulation has been reported to suppress the cell cycle, through the induction of the expression of cell cycle inhibitor proteins, including p21Cip/Waf and p27KIP [Marshall, 1999]. However, further investigations are required to understand the molecular mechanisms involved in the ERK-dependent cell death of SPC-treated cells.

In the present study, the SPC-induced cell death and activation of ERK were prevented by pretreatment of the cells with NAC. However, treatment of MS1 cells with U0126 did not abolish the SPC-induced generation of ROS, suggesting that the SPC-stimulated ROS generation is required for the SPC-induced ERK activation and concomitant cell death. Consistent with our present study, it has been reported that ROS-dependent activation of ERK is involved in cell death of various cell types [Ramachandiran et al., 2002; Chu et al., 2004; Clausen et al., 2004; Lee et al., 2005a,b]. Furthermore, ROS generation supports sustained MAPK activation via the inhibition of CD45 and other tyrosine phosphatases, and also contributes to the induction of distinct MAPK activation profiles via differential signaling pathways [Lee and Esselman, 2002; Zhou et al., 2002]. Therefore, these studies support our current data that ROS-mediated activation of MEK-ERK signaling pathways contributes to SPC-induced cell death in MS1 and HUVECs endothelial cells.

By using matrix-assisted laser desorption ionization-time-of-flight MS, the concentration of SPC was estimated at 50 nM in plasma and 130 nM in serum [Liliom et al., 2001]. We observed that SPC-induced apoptosis of MS1 cells and HUVECs at a higher concentration than 10 µM (Figs. 1A and 6). Consistent with the present study, SPC has been reported to affect proliferation in the micromolar range of SPC on several other cell types [Desai et al., 1993; Wakita et al., 1998]. Since these concentrations of SPC are higher than that found in plasma [Liliom et al., 2001], the physiological relevance of SPC-induced cell death can be argued. However, SPC is unlikely to act as a hormone but rather as a paracrine mediator in local microenvironments. Therefore, the concentration of SPC in local microenvironments could not be clearly determined and the physiological

and pathophysiological significance of the SPC-induced death of vascular endothelial cells should be investigated further.

REFERENCES

Alley MC, Scudiero DA, Monks A, Hursey ML, Czerwinski MJ, Fine DL, Abbott BJ, Mayo JG, Shoemaker RH, Boyd MR. 1988. Feasibility of drug screening with panels of human tumor cell lines using a microculture tetrazolium assay. Cancer Res 48:589–601.

Bass DA, Parce JW, Dechatelet LR, Szejda P, Seeds MC, Thomas M. 1983. Flow cytometric studies of oxidative product formation by neutrophils: A graded response to membrane stimulation. J Immunol 130:1910–1917.

Bektas M, Barak LS, Jolly PS, Liu H, Lynch KR, Lacana E, Suhr KB, Milstien S, Spiegel S. 2003. The G protein-coupled receptor GPR4 suppresses ERK activation in a ligand-independent manner. Biochemistry 42:12181–12191.

Boguslawski G, Lyons D, Harvey KA, Kovala AT, English D. 2000. Sphingosylphosphorylcholine induces endothelial cell migration and morphogenesis. Biochem Biophys Res Commun 272:603–609.

Cai H. 2005. Hydrogen peroxide regulation of endothelial function: Origins, mechanisms, and consequences. Cardiovasc Res 68:26–36.

Canals S, Casarejos MJ, de Bernardo S, Solano RM, Mena MA. 2003. Selective and persistent activation of extracellular signal-regulated protein kinase by nitric oxide in glial cells induces neuronal degeneration in glutathione-depleted midbrain cultures. Mol Cell Neurosci 24:1012–1026.

Chang L, Karin M. 2001. Mammalian MAP kinase signalling cascades. Nature 410:37–40.

Chin TY, Chueh SH. 1998. Sphingosylphosphorylcholine stimulates mitogen-activated protein kinase via a Ca^{2+}-dependent pathway. Am J Physiol 275:C1255–C1263.

Chu CT, Levinthal DJ, Kulich SM, Chalovich EM, DeFranco DB. 2004. Oxidative neuronal injury. The dark side of ERK1/2. Eur J Biochem 271:2060–2066.

Clair T, Aoki J, Koh E, Bandle RW, Nam SW, Ptaszynska MM, Mills GB, Schiffmann E, Liotta LA, Stracke ML. 2003. Autotaxin hydrolyzes sphingosylphosphorylcholine to produce the regulator of migration, sphingosine-1-phosphate. Cancer Res 63:5446–5453.

Clausen F, Lundqvist H, Ekmark S, Lewen A, Ebendal T, Hillered L. 2004. Oxygen free radical-dependent activation of extracellular signal-regulated kinase mediates apoptosis-like cell death after traumatic brain injury. J Neurotrauma 21:1168–1182.

de Bono DP, Yang WD. 1995. Exposure to low concentrations of hydrogen peroxide causes delayed endothelial cell death and inhibits proliferation of surviving cells. Atherosclerosis 114:235–245.

Desai NN, Spiegel S. 1991. Sphingosylphosphorylcholine is a remarkably potent mitogen for a variety of cell lines. Biochem Biophys Res Commun 181:361–366.

Desai NN, Carlson RO, Mattie ME, Olivera A, Buckley NE, Seki T, Brooker G, Spiegel S. 1993. Signaling pathways for sphingosylphosphorylcholine-mediated mitogenesis in Swiss 3T3 fibroblasts. J Cell Biol 121:1385–1395.

Fukunaga K, Miyamoto E. 1998. Role of MAP kinase in neurons. Mol Neurobiol 16:79–95.

Jeon ES, Kang YJ, Song HY, Im DS, Kim HS, Ryu SH, Kim YK, Kim JH. 2005a. Sphingosylphosphorylcholine generates reactive oxygen species through calcium-, protein kinase Cdelta- and phospholipase D-dependent pathways. Cell Signal 17:777–787.

Jeon ES, Kang YJ, Song HY, Woo JS, Jung JS, Kim YK, Kim JH. 2005b. Role of MEK-ERK pathway in sphingosylphosphorylcholine-induced cell death in human adipose tissue-derived mesenchymal stem cells. Biochim Biophys Acta 1734:25–33.

Jeon ES, Song HY, Kim MR, Moon HJ, Bae YC, Jung JS, Kim JH. 2006. Sphingosylphosphorylcholine induces proliferation of human adipose tissue-derived mesenchymal stem cells via activation of JNK. J Lipid Res 47:653–664.

Jiang X, Wang X. 2004. Cytochrome C-mediated apoptosis. Annu Rev Biochem 73:87–106.

Kalechman Y, Longo DL, Catane R, Shani A, Albeck M, Sredni B. 2000. Synergistic anti-tumoral effect of paclitaxel (Taxol) + AS101 in a murine model of B16 melanoma: Association with ras-dependent signal-transduction pathways. Int J Cancer 86:281–288.

Kim GS, Hong JS, Kim SW, Koh JM, An CS, Choi JY, Cheng SL. 2003. Leptin induces apoptosis via ERK/cPLA2/cytochrome c pathway in human bone marrow stromal cells. J Biol Chem 278:21920–21929.

Kim KS, Ren J, Jiang Y, Ebrahem Q, Tipps R, Cristina K, Xiao YJ, Qiao J, Taylor KL, Lum H, Anand-Apte B, Xu Y. 2005. GPR4 plays a critical role in endothelial cell function and mediates the effects of sphingosylphosphorylcholine. FASEB J 19:819–821.

Kimura T, Watanabe T, Sato K, Kon J, Tomura H, Tamama K, Kuwabara A, Kanda T, Kobayashi I, Ohta H, Ui M, Okajima F. 2000. Sphingosine 1-phosphate stimulates proliferation and migration of human endothelial cells possibly through the lipid receptors, Edg-1 and Edg-3. Biochem J 348(Pt 1):71–76.

Lee K, Esselman WJ. 2002. Inhibition of PTPs by H_2O_2 regulates the activation of distinct MAPK pathways. Free Radic Biol Med 33:1121–1132.

Lee ER, Kang YJ, Kim JH, Lee HT, Cho SG. 2005a. Modulation of apoptosis in HaCaT keratinocytes via differential regulation of ERK signaling pathway by flavonoids. J Biol Chem 280:31498–31507.

Lee WC, Choi CH, Cha SH, Oh HL, Kim YK. 2005b. Role of ERK in hydrogen peroxide-induced cell death of human glioma cells. Neurochem Res 30:263–270.

Lieu CH, Liu CC, Yu TH, Chen KD, Chang YN, Lai YK. 1998. Role of mitogen-activated protein kinase in taxol-induced apoptosis in human leukemic U937 cells. Cell Growth Differ 9:767–776.

Liliom K, Sun G, Bunemann M, Virag T, Nusser N, Baker DL, Wang DA, Fabian MJ, Brandts B, Bender K, Eickel A, Malik KU, Miller DD, Desiderio DM, Tigyi G, Pott L. 2001. Sphingosylphosphocholine is a naturally occurring lipid mediator in blood plasma: A possible role in regulating cardiac function via sphingolipid receptors. Biochem J 355:189–197.

Lin SJ, Shyue SK, Liu PL, Chen YH, Ku HH, Chen JW, Tam KB, Chen YL. 2004. Adenovirus-mediated over-expression of catalase attenuates oxLDL-induced apop-

tosis in human aortic endothelial cells via AP-1 and C-Jun N-terminal kinase/extracellular signal-regulated kinase mitogen-activated protein kinase pathways. J Mol Cell Cardiol 36:129–139.

Ludwig MG, Vanek M, Guerini D, Gasser JA, Jones CE, Junker U, Hofstetter H, Wolf RM, Seuwen K. 2003. Proton-sensing G-protein-coupled receptors. Nature 425: 93–98.

Marshall C. 1999. How do small GTPase signal transduction pathways regulate cell cycle entry? Curr Opin Cell Biol 11:732–736.

Meyer zu Heringdorf D, Himmel HM, Jakobs KH. 2002. Sphingosylphosphorylcholine-biological functions and mechanisms of action. Biochim Biophys Acta 1582:178–189.

Murakami N, Yokomizo T, Okuno T, Shimizu T. 2004. G2A is a proton-sensing G-protein coupled receptor antagonized by lysophosphatidylcholine. J Biol Chem 279: 42484–42491.

Nguyen TT, Tran E, Nguyen TH, Do PT, Huynh TH, Huynh H. 2004. The role of activated MEK-ERK pathway in quercetin-induced growth inhibition and apoptosis in A549 lung cancer cells. Carcinogenesis 25:647–659.

Nofer JR, Levkau B, Wolinska I, Junker R, Fobker M, von Eckardstein A, Seedorf U, Assmann G. 2001. Suppression of endothelial cell apoptosis by high density lipoproteins (HDL) and HDL-associated lysosphingolipids. J Biol Chem 276:34480–34485.

Nofer JR, van der GM, Tolle M, Wolinska I, von Wnuck LK, Baba HA, Tietge UJ, Godecke A, Ishii I, Kleuser B, Schafers M, Fobker M, Zidek W, Assmann G, Chun J, Levkau B. 2004. HDL induces NO-dependent vasorelaxation via the lysophospholipid receptor S1P3. J Clin Invest 113:569–581.

Ohba M, Shibanuma M, Kuroki T, Nose K. 1994. Production of hydrogen peroxide by transforming growth factor-beta 1 and its involvement in induction of egr-1 in mouse osteoblastic cells. J Cell Biol 126:1079–1088.

Ramachandiran S, Huang Q, Dong J, Lau SS, Monks TJ. 2002. Mitogen-activated protein kinases contribute to reactive oxygen species-induced cell death in renal proximal tubule epithelial cells. Chem Res Toxicol 15: 1635–1642.

Schulze PC, Lee RT. 2005. Oxidative stress and atherosclerosis. Curr Atheroscler Rep 7:242–248.

Seo SR, Chong SA, Lee SI, Sung JY, Ahn YS, Chung KC, Seo JT. 2001. Zn^{2+}-induced ERK activation mediated by reactive oxygen species causes cell death in differentiated PC12 cells. J Neurochem 78:600–610.

Stanciu M, Wang Y, Kentor R, Burke N, Watkins S, Kress G, Reynolds I, Klann E, Angiofieri MR, Johnson JW, DeFranco DB. 2000. Persistent activation of ERK contributes to glutamate-induced oxidative toxicity in a neuronal cell line and primary cortical neuron cultures. J Biol Chem 275:12200–12206.

Stoneman VE, Bennett MR. 2004. Role of apoptosis in atherosclerosis and its therapeutic implications. Clin Sci (Lond) 107:343–354.

Sun L, Xu L, Henry FA, Spiegel S, Nielsen TB. 1996. A new wound healing agent—sphingosylphosphorylcholine. J Invest Dermatol 106:232–237.

Touyz RM, Schiffrin EL. 2004. Reactive oxygen species in vascular biology: Implications in hypertension. Histochem Cell Biol 122:339–352.

Wada T, Penninger JM. 2004. Mitogen-activated protein kinases in apoptosis regulation. Oncogene 23:2838–2849.

Wakita H, Matsushita K, Nishimura K, Tokura Y, Furukawa F, Takigawa M. 1998. Sphingosylphosphorylcholine stimulates proliferation and upregulates cell surface-associated plasminogen activator activity in cultured human keratinocytes. J Invest Dermatol 110: 253–258.

Wang F, Van Brocklyn JR, Hobson JP, Movafagh S, Zukowska-Grojec Z, Milstien S, Spiegel S. 1999. Sphingosine 1-phosphate stimulates cell migration through a G_i-coupled cell surface receptor. Potential involvement in angiogenesis. J Biol Chem 274:35343–35350.

Xia Z, Dickens M, Raingeaud J, Davis RJ, Greenberg ME. 1995. Opposing effects of ERK and JNK-p38 MAP kinases on apoptosis. Science 270:1326–1331.

Xu Y. 2002. Sphingosylphosphorylcholine and lysophosphatidylcholine: G protein-coupled receptors and receptor-mediated signal transduction. Biochim Biophys Acta 1582:81–88.

Xu Y, Casey G, Mills GB. 1995a. Effect of lysophospholipids on signaling in the human Jurkat T cell line. J Cell Physiol 163:441–450.

Xu Y, Fang XJ, Casey G, Mills GB. 1995b. Lysophospholipids activate ovarian and breast cancer cells. Biochem J 309(Pt 3):933–940.

Yamada T, Okajima F, Ohwada S, Kondo Y. 1997. Growth inhibition of human pancreatic cancer cells by sphingosylphosphorylcholine and influence of culture conditions. Cell Mol Life Sci 53:435–441.

Zhou B, Wang ZX, Zhao Y, Brautigan DL, Zhang ZY. 2002. The specificity of extracellular signal-regulated kinase 2 dephosphorylation by protein phosphatases. J Biol Chem 277:31818–31825.